Viscoelastic and light scattering studies on thermally induced sol to gel phase transition in fish myosin solutions

Sawa Kouchi[1], Shingo Kondo[1], Kazuko Ooi[1], Hisashi Ichikawa[2] and Toshiaki Dobashi[1],

[1]Department of Biological and Chemical Engineering, Faculty of Engineering, Gunma University, Kiryu, Gunma 376-8515, Japan
[2]Division of Advanced Materials, Graduate School of Science and Engineering, Nagasaki University, Nagasaki 852-8521, Japan

Keywords: fish myosin; thermally induced gelation; viscoelasticity; dynamic light scattering

Correspondence to : T. Dobashi; e-mail dobashi@bce.gunma-u.ac.jp

Abstract

Viscoelastic (VE) and dynamic light scattering (DLS) analyses of fish (white croaker) myosin solutions were performed at myosin concentrations of 30mg/ml for VE and 0.1mg/ml for DLS at 0.6 MKCl and pH 7.0 to clarify thermally induced gelation. The hydrodynamic radius R_h considerably decreased around 30-35°C. The shear modulus G was constant below 25°C and increased by incubating the sample at 30°C. G further increased as the temperature of the incubated sample decreased. The curves of G vs. T for different time courses showed a sharp peak around 35°C and a moderate peak around 60°C in the heating process, while a stepwise increase in G was observed around 30°C in the cooling process when the temperature was elevated to not more than 60°C. No distinct stepwise change was observed once the temperature of the sample exceeded 60°C. The absolute value of G strongly depended on the maximum elevated temperature and the incubation time at that temperature. The corresponding behavior of the viscosity η was observed for each time course. Based on these results, the mechanism of thermally induced gelation of myosin solutions is discussed in view of S-S bridge formation in the head and tail portions and unwinding/rewinding of coiled-coil α-helices in the tail portion.

Introduction

Fish muscle myosin (myosin II) molecules have ATPase activity, actin-binding activity on the globular head portion and filament-forming ability on the coiled coil tail portion, just like mammalian muscle myosin molecules,[1,2] but they are easily denaturated by heating. Johnston and Goldspink showed a strong positive correlation of both activation entropy and enthalpy for myofibrillar ATPase reaction with the mean annual habitat temperature of the species, while activation free energy remains roughly constant.[3] They suggested that the higher order structures of myofibrillar proteins are destabilized to enable fish to adapt a wide range of thermal environments from Antarctic to tropical waters. This characteristic thermodynamic property has been attributed to the main component of myofibrils, namely, myosin. The denaturation temperature of myosin is also known to depend on the environmental temperature of the fish species.[4] In association with the denaturation of the myosin molecules, the viscoelastic properties of the myosin solution considerably change. This phenomenon has been utilized to obtain many kinds of fish paste gel in food industry.[5] Thus, investigation of the mechanism of the thermally induced change of fish myosin solutions is crucial from both biological and industrial aspects.

The gel strength g of fish paste significantly depends on the fish species, as well as the location where and the season when the fish was captured, while some characteristic features of g are always observed: an increase in g at low temperatures of 10-30^{o}C, a decrease in g at moderate temperatures of 40-60^{o}C and an increase in g at high temperatures around 80^{o}C.[5] Generally, the gelation of myosin solutions has been attributed to the aggregation of the myosin head and/or twisting of the coiled coil myosin tail by both physical cross-linking due to hydrogen bonding, ionic bonding or hydrophobic bonding

and chemical cross-linking due to S-S bonding.[6,7] It is considered that heating myosin solutions induces oxidation of the SH group;[8] myosin dimers are formed at temperatures lower than 40°C and star-like multimers are formed between the heads at temperatures higher than 40°C.[9] It was also pointed out that S-S bridges are not formed between the head and the tail of a single myosin molecule,[8] and highly ordered water is important for the formation of myosin gel.

By using circular dichroism and cDNA cloning technique, Ojima et al. [10] reported recently reversible unfolding of 2/3 of light meromyosin (LMM) from the N-terminal and irreversible unfolding of 1/3 of LMM from the C-terminal of walleye pollack myosin on heat treatment. Gel network formation, however, could not be induced by heating LMM. Thus, it is interesting to study the relationship between such molecular level information and macroscopic viscoelasticity. However, detailed studies reported to date are quite few except for those of animal meat.[6,7] For example, it is still controversial whether the heating process or the cooling process is essential to gelation.[11] To discriminate the reversible part and the irreversible part of the thermally induced gelation process, it is required to investigate both heating and cooling processes. In a previous study, we reported that the curve for shear modulus G vs. temperature T showed a peak around T_1=36°C in the heating process and a drastic increase around T_2=31°C, indicating sol to gel transition in the cooling process, independent of myosin concentration.[12] This result suggests that the thermally induced viscoelastic behavior is affected by the history of the treatment of the sample and the origin of the change is attributed to a conformational change of a single myosin molecule. One of the experimental difficulties in the study of this subject is that it is difficult to include a wide enough range of myosin concentration; for example,

concentrated solutions cannot be studied by light scattering because of high turbidity, and dilute solutions cannot be studied by viscoelasticity because of low precision. In this study, to clarify the mechanism of the change of the myosin solution structure on heat treatment, we performed experiments by combining two techniques: dynamic light scattering for dilute myosin solution and viscoelastic analysis for concentrated solutions, which could provide us information at both molecular and macroscopic levels.

Experiments

A. Sample

The dorsal epaxial muscle of the white croaker (*Pennahia argentata*) from Tachibana bay at Mogi harbor in Nagasaki Prefecture was minced in seven-fold 19 mM sodium phosphate buffer at pH 7.5, homogenized for 60 min and centrifuged at 500×g for 10 min. This process was repeated twice and the supernatant was removed. Threefold buffer solution containing 2 mM ATP, 2 mM $MgCl_2$, 0.45 M KCl, and 67 mM sodium phosphate at pH 6.4 was added to the precipitates. After gently stirring the solution for 10 min and centrifuging it at 6,000×g for 15 min, the supernatant was filtered through 2-3 sheets of nylon gauze. The filtrate was poured into fourteenfold cold deionized water and allowed to settle at 5 °C for 10 min. Proteins were collected by centrifuging the precipitates that appeared at the bottom of the vessel at 6,000×g for 10 min (dilution precipitation). The proteins were dissolved in 1/3-fold buffer solution containing 3 M KCl and 0.25 M Tris-HCl at pH 7.0. KCl concentration was adjusted to 0.6 M by adding the desired amount of cold deionized water. Then, to the solution were added 2 mM ATP and 50 mM $MgCl_2$, and this was ultracentrifuged at 100,000×g for 60 min to remove the precipitates. Final myosin solution was obtained by repeating

the dissolution and the dilution precipitation. From electrophoresis with sodium dodecyl sulfate contained-10% polyacrylamide gel, the percentage weight of myosin, actin, tropomyosin, troponin and others was determined as 95 %, ND, ND, ND and 5 %, respectively. Salt concentration was fixed at 0.6 M KCl and 50 mM Tris-HCl (pH 7.0). Myosin solutions with the concentrations c = 30 mg/ml and 0.1mg/ml were prepared for viscoelastic study and light scattering study, respectively. The sample for light scattering was filtered through a 0.2 μm Millipore filter just before the experiment.

B. Measurements

Dynamic light scattering experiment was performed using a laboratory-made light scattering apparatus.[13] Green diode laser (BWT-50, B&W) operating at 532 nm with an output power of 50 mW was used. The sample cell was immersed in a silicone bath, the temperature of which was controlled to ±0.02 °C. The intensity autocorrelation function $G^{(2)}(t)$ was measured at the scattering angle of 90° with a Brookhaven BI-9000 correlator. $G^{(2)}(t)$ has the form[14]

$$G^{(2)}(t)=A(1+\beta|g^{(1)}(t)|^2), \qquad (1)$$

where t is the delay time; A, the baseline; β, the spatial coherence factor; and $g^{(1)}(t)$, the first-order normalized electric field time correlation function, which is related to the normalized characteristic line width Γ distribution function $G(\Gamma)$ by the Laplace transformation:

$$g^{(1)}(t)=\int G(\Gamma)\exp(-\Gamma t)d\Gamma \qquad (2)$$

Data analysis was performed by using the CONTIN method[15] in order to obtain an average line width Γ defined by $\int \Gamma G(\Gamma)d\Gamma$. The z-average translational diffusion coefficient D was calculated from the equation $D=\Gamma/q^2$.

The average hydrodynamic radius R_h was estimated by using the Stokes-Einstein equation $R_h=k_BT/(6\pi\eta D_0)$, where k_B is the Boltzmann constant; T, the absolute temperature; η, the solvent viscosity; and D_0, the diffusion coefficient extrapolated to zero concentration. Here, D_0 was approximated from D measured for 0.1 % myosin solution. The time course of the experiment is shown in Fig. 1(a); 25°C– 35°C – 45°C – 35°C– 25°C – 17°C – 4°C(11h)– 25°C – 35°C – 45°C– 60°C, where the time in parentheses is the incubation time.

Rheological measurement was performed with a Rhesca Model RD-100 AD coaxial cylinder-type torsional viscoelastometer.[16] 3 ml of myosin solution was poured between the outer cylinder (Pyrex tube with 14.4 mm i.d.) and the inner cylinder (stainless steel rod covered with Pyrex tube with 8 mm o.d.) and set in an air bath in the apparatus. By rotating the inner cylinder up to the shear angle of 0.25°, a freely damping oscillation was induced by elastic restoring force of the sample and a piano wire supporting the inner cylinder. From the damping oscillation curve after the shear angle became less than 0.2°, the shear modulus G and the viscosity coefficient η were calculated by

$$\alpha_T = \ln\theta_0/\theta_1 = \ln\theta_1/\theta_2 = \cdots = (1/n)(\ln\theta_0/\theta_n)$$

$$\kappa = 4\pi^2 I/T_d^2 - k_0$$

$$R = (2\alpha_T/T_d)\, I$$

$$G = \kappa/4\pi l\,(1/r_1^2 - 1/r_2^2)$$

$$\eta = R/4\pi l\,(1/r_1^2 - 1/r_2^2).$$

The notations are as follows:

α_T : logarithmic decrement, θ_i : amplitude of ith wave, κ : rigidity coefficient,

I: moment of inertia, T_d: period, k_0: piano wire constant, R: viscosity constant, G : shear modulus, l : length of the region where the sample and the inner cylinder are in contact, r_1 : outer diameter of inner cylinder, r_2 : inner diameter of outer cylinder, η : viscosity coefficient, n : order of vibration.

The viscoelasticity of myosin solutions was measured using the inner cylinder with 8 mm o.d. Measurements were performed in five different time courses as shown in Fig. 1(b); Time course 0, room temperature (rt) at 22°C– 0°C –rt; Time course I, rt – 30°C (16.7h) – 0°C – 45°C (1.7h) – 0°C – 45°C – rt; Time course II, rt – 45°C (2.6h) – 0°C – 60°C (1.8h) –0°C – 60°C; Time course III, rt – 80°C (3.3h) – 0°C –80°C – 45°C; Time course IV, rt – 95°C – 0°C – 95°C – 55°C, where the time in parentheses denotes the incubation time. The temperature scanning rate was 0.35 °C/min in both heating and cooling processes.

Results

Figure 2 shows the average hydrodynamic radius R_h of myosin molecules as a function of T for the time course shown in Fig. 1(a). It is noticeable that R_h considerably changes in the temperature range of 25 to 35°C. When the temperature of the untreated sample is raised above 30-35°C, R_h decreases by about 30 nm (broken line). Thereafter, the values of R_h obtained at the same temperature at different times, i.e., (G, E), (B, D, H) and (I, C) agree with each other within the experimental precision of ± 4 nm. These results indicate that the thermal behavior of R_h of myosin molecules treated once at 30-35°C is reversible with a variation of 15 nm around 30-35°C in the experimental temperature range of 17°C to 45°C. This suggests that a conformational change such as rod-like to Gaussian of myosin molecules occurs around 35°C.

Figures 3-6 show the shear modulus G (a) and the viscosity coefficient η (b) for the five different time courses 0-IV shown in Fig. 1(b). The inset in Fig. 3 shows the results of the experiment performed at time course 0. G slightly decreases and η increases with decreasing temperature below room temperature, which corresponds to those of pure water. Figure 3 shows the result for the experiment performed at time course I. G increases from 4.6 to 46 Pa by incubating the sample at 30°C (○) (pre-heating). By decreasing the temperature to 0°C (the first cooling process (▼)), G further increases to 90 Pa. By increasing the temperature again (the first heating process (△)), G decreases through the same path as the first cooling process up to 30°C, then increases up to 35°C and decreases again up to 45°C, i.e., the curve for the heating process has a peak around 35°C. In the second cooling process (■) G increases abruptly around 35°C and further increases linearly depending on the temperature with a small depression around 20°C. G at 0°C in the second process is three times more than that in the first process. In the second heating process (□), G decreases through a path roughly parallel to the second cooling process; nevertheless, about 30 Pa higher than that in the second cooling process. In both the first and the second processes, a hysteresis is observed between the cooling and heating processes, especially near 35°C. In the third cooling process (◆), G passes through the same path as that in the second cooling process (■). G at 45°C in the second heating process is 20% larger than that in the first heating process. The viscosity coefficient η shows a corresponding complex behavior with G, as shown in Fig. 3 (b). η increases exponentially with time from 0.3 to 1.6 Pa s, when the sample is incubated at 30°C (○). In the first cooling process (▼), η decreases from 30°C to 24°C and increases from 24 °C to 0 °C with a shoulder around 20 °C. As the temperature is increased (the first heating process

(△)), η decreases through a path roughly parallel to the first cooling process up to 30°C, increases again up to 37°C and decreases up to 45°C, i.e., the curve for the heating process has a minimum around 30°C and a maximum around 37°C, the peak height of which is 3.5 Pa s. In the second cooling process (■), η shows a sharp peak around 33°C just like in the first heating process and a minimum around 25°C, the height of which is roughly twice as that in the first process, and increases again down to 0°C with a shoulder around 20°C. η at 0°C in the second process is 17% larger than that in the first process. In the second heating process (□), the curve for η passes through the same path as that in the second cooling process. In both the first and second processes, a hysteresis is observed like in G, especially near the shoulder around 20°C and the maximum around 35°C. η in the third cooling process (◆) agrees with that in the second cooling process.

Figure 4 shows the results of the experiment performed at time course II. The curves for G and η in time course II are essentially the same as those in time course I. The characteristic feature is summarized as follows: In the pre-heating from room temperature to 45°C (○), the peak of G is observed around 35°C; the temperature dependence of η for the first cooling (▼) and heating (△) processes is similar to that in time course I but the absolute value is 30% lower than that in time course I; the hysteresis observed around 35°C is much clearer than that in time course I. G increases from 10 to 27 Pa when incubating the sample at 60°C, which is much larger than the increase from 1.5 to 3.3 Pa when incubating it at 45°C. In the second cooling process (■), a similar increase in G to that in the first cooling process (▼) is observed, but a stepwise change around 35°C becomes vague and a small lag appears around 15°C. G in the second heating process (□) is larger than that in the second cooling process (■) in the range of 0°C to 15°C and of 35°C to 60°C and

no lag or shoulder is found around 15°C or 20°C in the curve. In the pre-heating (○), the curve of η vs. T has a sharp peak around 38°C. η increases from 0.3 to 11 Pa s at the peak. In the first cooling process (▼), a maximum appears in the curve around 33°C and a minimum appears around 25°C with a shoulder around 30°C. η at the peak around 33°C is 4 Pa s, which is much smaller than that in the pre-heating process (○). In the first heating process (△) η decreases via a similar path to that in the first cooling process (▼), but a clear hysteresis is observed; η in the first heating process (△) is shifted to a higher temperature than that in the first cooling process(▲) by the shift of the peak. In the second cooling process (■), η has a moderate peak around 55°C, a maximum around 35°C, a minimum around 25°C and a shoulder around 20°C. The peak around 35°C becomes smaller than that in the first process. The curve η vs. T in the second heating process (□) passes through a similar path to that in the second cooling process (■) up to 35°C.

Figure 5 shows the results of the experiment performed at time course III. The curve of G vs. T has a similar peak around 35°C in the pre-heating process (○) to that in time courses I and II, although the peak is difficult to recognize in Fig. 5(a) because the peak height of G = 50 Pa is much smaller than the maximum value of G = 7000 Pa in the plot. G increases monotonically with decreasing temperature in the first cooling process (▼) and has a shallow minimum around 45°C in the first heating process (△), but no abrupt change corresponding to a phase transition is observed. G in the first heating process (△) is larger in the range of 0°C to 18°C and of 40°C to 80°C and smaller in the range of 18°C to 40°C than that in the first cooling process (▼). In the curve of η vs. T for pre-heating (○), a peak is observed around 38°C, similar to those in the time courses I and II. A moderate peak

is observed around 55°C in the first cooling process (▼) and a broader peak, in the first heating process (△).

Figure 6 shows the results of the experiment performed at time course IV. The behaviors of G and η are essentially the same as those in time course III, except that we can hardly observe a broad peak around 35°C. This is because of the difference in the scale of the ordinate between Fig. 6 and Figs. 3, 4 and 5. The process is completely irreversible, as shown in Figs. 6 (a) and (b).

Figure 7 shows G and η at 25°C and 40°C as a function of the highest elevated temperature of the sample, T^*. No significant difference in G and η is found between the cooling process and the heating process except at 90°C. From the difference at 90°C, it is suggested that complex chemical reactions are activated. The higher the temperature, the larger the increments in G and η are.

The results of viscoelastic measurements are summarized as follows. (1) The temperature dependence of the viscoelasticity of myosin solutions is essentially set by the highest elevated temperature T^*. (2) For $T^* \lesssim$ 25°C, no significant behavior was observed for the sample kept at T^*. (3) For T^*~30°C, an irreversible increase of G and η occurs by incubating the sample at relatively low temperatures of T^*, and G and η increase roughly linearly by decreasing the temperature. (4) For T^*=45°C, a hysteresis around 30-45°C and a shoulder around 20°C are observed in the curve for G and more obviously in the curve for η in samples with T^* (time courses I and II). (5) For T^*=60°C, a small lag in G around 15°C and a small peak of η around 55°C appear in the cooling process, and the hysteresis is explicit only below 10°C (time course II). (6) As T^* is higher and the incubation time at T^* is longer, the hysteresis around 35°C, the shoulder around 20°C and a lag around 15°C become vague. When $T^* \gtrsim$ 60°C, a stepwise change in G around 35°C

disappears and the trace of the lag in G around 15°C in the cooling process remains unclear, while the peak or the shoulder of η around 55°C is clear in the heating process.

Discussion

The kinetic progress of biopolymer gelation has been studied with several network theories.[17-19] Nishinari et al. classified the temperature dependence of the elastic modulus G of gel in three types using a zipper model;[19] when the distance between the cross-links and the number of segments consisting a cross-link is assumed to be constant, G increases with temperature when the energy for forming a cross-linking ε is small, such as arabic gum, G decreases with temperature when ε is large, such as carrageenan and gelatin, and G has a maximum when ε is intermediate, such as vinyl alcohol and agarose. The present experimental results for light scattering and viscoelastic measurements could be discussed on the basis of these theoretical results. The sharp increases in G and η around 35°C in the cooling process are similar to the phenomena characteristic to the viscoelasticity change in the sol to gel phase transition of biopolymer solutions. From the anomaly of R_h around 30-35°C in Fig. 2, the peak of G around 35°C in Figs.3 and 4 must be related to a conformational change of myosin molecules. If we presume breakings of hydrogen bonds in myosin molecules by increasing the temperature above 30°C and forming of hydrogen bonds between different myosin molecules by lowering the temperature, the findings of the sharp increase in G around 35°C associated with the sol to gel transition and the negative slope of the G vs. T curve in the gel phase (below 30°C) in the cooling process are consistent with the theory of Nishinari et al.

Thus, the elastic behaviors of our system could be described qualitatively

by Nishinari et al.'s general model. However, molecular parameters vary considerably with T* and the procedures to fit their model to the present experimental results by considering the characteristics of myosin molecules may be complicated. Instead of the direct application of the Nishinari's model, we try to treat the reversible process first, that is, the linear dependence of G on (-T), which is thought to be the most essential, by using the following simplified molecular model.

When the temperature is raised to less than the gel-sol transition point around 35°C, we assume that the α-helices in myosin molecules are only partly transformed into random coils; then, S-S bridges are not formed at the tail portions[8] and entanglements with different chains are negligible. In this case, the gel structure is produced by connecting the head portions of different molecules by S-S bonding and the tail portion of each molecule by keeping the coiled coil structure. Let us consider a myosin molecule incubated around 40°C with the distance between the cross-links being extended from L to $L+\Delta L$ by an external force K' (see Fig. 8). The network chains consist of S-S bridges on the head (cross-link) and the coiled coil on the tail, forming partly α-helices and partly random coil chains. We further assume a force acting perpendicular to the coiled coil axis at the branched point A in Fig. 8 as K_c, which is the force required to keep the length of the coiled coil portion to a certain constant value. We denote the end-to-end distance of the two heads being free by fixing the length of the coiled coil portion as l, and the force required to extend the end-to-end distance by unit length from l as c at arbitrary temperature T. Then, the force balance equation is $(L-l)c=K_c$. This means that in the network at an equilibrium state, the external forces acting on the two heads must have a component with a magnitude of K_c in the direction connecting the two heads. In the myosin solutions, it may be

reasonable to assume that the time scale to alter the length of the coiled coil portion is long enough in comparison with that of molecular motions. Supposing that an external force K' is required to act on the two heads inversely along the direction connecting them when the end-to-end distance is increased by ΔL from L, the following relationship holds among the variables:

$\Delta K=K'-K_c = (L+\Delta L-l)c-(L-l)c = c\Delta L = cL\Delta L/L = cL\varepsilon$.

Thus, stress σ is expressed as $\sigma=\kappa\varepsilon$, where $\kappa=cL/\gamma=(K_c+lc)/\gamma$ and γ is a constant related to the structure of the solution. For Gaussian chains, $l=0$ and we obtain the elastic modulus as $\kappa=K_c/\gamma$.

We assume that the coiled coil begins to form at critical temperature T_c and energy E_c is required to unfold the coiled coil or α-helix. We also assume that force K_c generated by the thermal motion of molecules is exerted at both ends of the network for unfolding the coiled coil at arbitrary temperatures below T_c up to that at T_c. Then, we have

$\exp(-E_c/kT_c)=\exp\{-(E_c-K_c\Delta\rho)/kT\}$ or $K_c=E_c(1-T/T_c)/\Delta\rho$,

where $\Delta\rho$ is a displacement for the activation. Here we assume that the energy to form the helix or coiled coil does not depend on the chain length and the change of the interaction between chains and solvent associated with the temperature change can be included in the change in K_c. Thus, the temperature dependence of G in the system with T^*=45℃ is successfully represented. The deviations from the above model probably come from irreversible changes of the molecular chain structure.

The increase in G at relatively low temperatures may be closely related to the setting (*Suwari*)[5]; the increase in gel strength at low temperatures observed in fish meat. The values of G and η at 25°C and 40°C depended on the highest elevated temperature T^* and the incubation time of the sample at T^*. It seems that the gel memorized the network at T^*, i.e., the values of G

and η reflected the network once formed at T^*. The disappearance of clear hysteresis and sharp transition for the sample at high T^* might be attributed to the collapse of the higher order structure of myosin molecules.

Recently, the complete primary structure of the myosin heavy chain from white croaker fast skeletal muscle was investigated by cDNA cloning.[2] It is interesting to compare that with the primary structure of mammalian ones such as rabbit myosin.[20] The contents of the cysteine and glycine residues of white croaker myosin light meromyosin (LMM) are much larger than those of rabbit LMM, especially near the C-terminal of LMM. This may be closely related to the characteristic viscoelasticity in the sol to gel transition in the cooling process, since the cysteine residues form S-S bonds and the glycine residues can destabilize the coiled coil α-helical structure and contribute to increasing hydration. The thermally induced gelation mechanism itself should be not much different among hereditary related fish. Thus, it is interesting to investigate the location of cystein residues in the amino acid sequence. There are eleven cysteines in S1 and six cysteines in the tail portion (three in S2 and three in LMM) of white croaker myosin.[16] Ojima et al. reported that 2/3 of LMM from the N-terminal unfolds reversibly and 1/3 of LMM from the C-terminal unfolds irreversibly on heat treatment in the walleye pollack.[10] On the other hand, it is known that gel network formation cannot be induced by cooling LMM after incubation at high temperatures. Thus, S2 portion should also be necessary for inducing reversible gel formation. The reversible change of viscoelasticity for the sample incubated below 60°C and the irreversible change of viscoelasticity for the sample incubated at 80°C and 90°C may be attributed to S-S cross-linkings among S1 and S2 portions and those among LMM portions belonging to different myosin molecules, respectively.

From the above discussion, the mechanism of the thermally induced gelation of myosin solution is summarized, as shown in Fig. 9: As the temperature increases, the unfolding of the heavy chains of myosin molecules and the transformation from coiled coil α-helices to random chains are promoted in the tail portion, cysteine residues are exposed to the medium and intra- or intermolecular S-S bridges are formed in the head portion around 30-35°C. As the temperature is decreased, intramolecular and intermolecular refolding of the coiled coil α-helices takes place. This results in sol to gel transformation and an increase in G. When the samples are incubated at temperatures higher than 55-60°C, S-S bridges are also formed in the tail portion, and the network structure formed at high temperatures becomes complicated. Although it has been reported that a periodic charge distribution in the myosin rod amino acid sequence enables formation of the α-helix and the coiled coil structure,[20] the energy of formation of such structures at different sites is expected to be different from each other. In the cooling process, the portion of specific amino acid sequences that can form α-helix and coiled coil structure tends to fold in the order of high activation energy of the bond. Since measurements cannot be performed at the equilibrium state at each temperature in this measurement, the minimum free energy may not be reached. It is speculated that the quasistable structure is partly broken and changes itself to a more stable structure, and this may induce the shoulder or lag in G and η around 20°C.

References

1. Pearson, A. M.; Young, R. B. Proteins of the Thick Filament in Muscle and Meat Biochemistry; eds. by Pearson, A. M. and Young, R. B., Academic Press: London, 1989.
2. Yoon, S. H.; Kakinuma, M.; Hirayama, Y.; Yamamoto T.; Watabe, S. Fisheries Sci 2000, 66, 1163-1171.
3. Johnston, I. A.; Goldspink, G. Nature 1975, 257, 620-622.
4. Connell, J.J. Biochem J 1961, 80, 503-509.
5. Hall, G. M.; Ahmad, N. H. Surimi and fish-mince products in Fish Processing Technology; ed. by Hall, G. M. Blackie Academic & Professional: London, 1997.
6. Samejima, K.; Ishioroshi, M.; Yasui, T. J Food Sci 1981, 46, 1412-1418.
7. Ishioroshi, M.; Samejima, K.; Yasui, T. J Food Sci 1981, 47, 114-120.
8. Itoh, Y. Nippon Suisan Gakkaishi 2000, 66(3), 380-383.
9. Yamamoto, K. J Biochem 1990, 108, 896-898.
10. Ojima, T.; Higuchi, T.; Nishita, K. Fisheries Science 1999, 65(3), 459-465.
11. Arai, K. Nippon Suisan Gakkaishi 2002, 68, 137-143.
12. Ooi, K.; Kouchi, S.; Dobashi, T.; Kondo, S.; Ichikawa, H. Trans MRS-J 2001, 26(2), 605-608.
13. Isojima, T.; Fujii, S.; Kubota K.; Hamano, K. J Chem Phys 1999, 111, 9839-9846.
14. Siegert, A.J. MIT Rad. Lab Rep 1943, No.465.
15. Provencher, S.W. Makromol Chem 1979, 180, 201.
16. Kondo, S.; Igarashi, T.; Nakamura, T.; Okuizumi, T. Colloid Polym Sci 1983, 261, 819-824.
17. Clark, A. H.; Ross-Murphy, S. B. Adv Polym Sci 1987, 83, 57-192.
18. Clark, A. H. The Application of Network Theory to Food Systems: in Food

Structure and Behaviour, edited by Lillford P. J.; Blanshard, J. M. V. Academic Press: New York, 1987; pp13-34.

19. Nishinari, K.; Koide S.; Ogino, K. J Phys (Paris) 1985, 46, 793-797.
20. Boyer, C.; Joandel, S.; Ouali A.; Culioli, J. J Sci Food Agric 1996, 72, 367-375.
21. McLachlan A. D.; Karn, J Nature 1982, 299, 226.

Figure captions

Fig. 1 Time course of the experiments for light scattering (a) and viscoelasticity (b). The symbols (▽), (●), (□), (◆) and (△) correspond to Time course 0, I, II, III and IV, respectively.

Fig. 2 Average hydrodynamic radius as a function of temperature. The letters correspond to the times indicated by the same letter in Fig. 1(a).

Fig. 3 Shear modulus G (a) and viscosity coefficient η (b) for Time course I. Data were acquired in the order of (○),(▼),(△), (■), (□) and (◆). Inserted figure is the temperature dependence of G and η for Time course 0, where data were acquired in the order of (●) and (○).

Fig. 4 Shear modulus G (a) and viscosity coefficient η (b) for Time course II. Data were acquired in the order of (○),(▼),(△), (■) and (□).

Fig. 5 Shear modulus G (a) and viscosity coefficient η (b) for Time course III. Data were acquired in the order of (○),(▼) and (△).

Fig. 6 Shear modulus G (a) and viscosity coefficient η (b) for Time course IV. Data were acquired in the order of (○),(▼) and (△).

Fig. 7 Shear modulus G (a) and viscosity coefficient η (b) observed at 25°C in the heating process (△) and the cooling process (▼) and those observed at 40°C in the heating process (□) and the cooling process (■) as a function of the highest elevated temperature T^*.

Fig. 8　Schematic illustration of a myosin molecule. S is the point of mass in the head portion, K' the external force, A the branched point in the tail portion, $L+\Delta L$ the distance of the points of mass of two heads and K_c a constant force acting perpendicular to the coiled-coil axis at the branched point A.

Fig. 9　Schematic illustration of the change of the conformation of myosin molecules in concentrated solution by heating and cooling treatment.

(a)

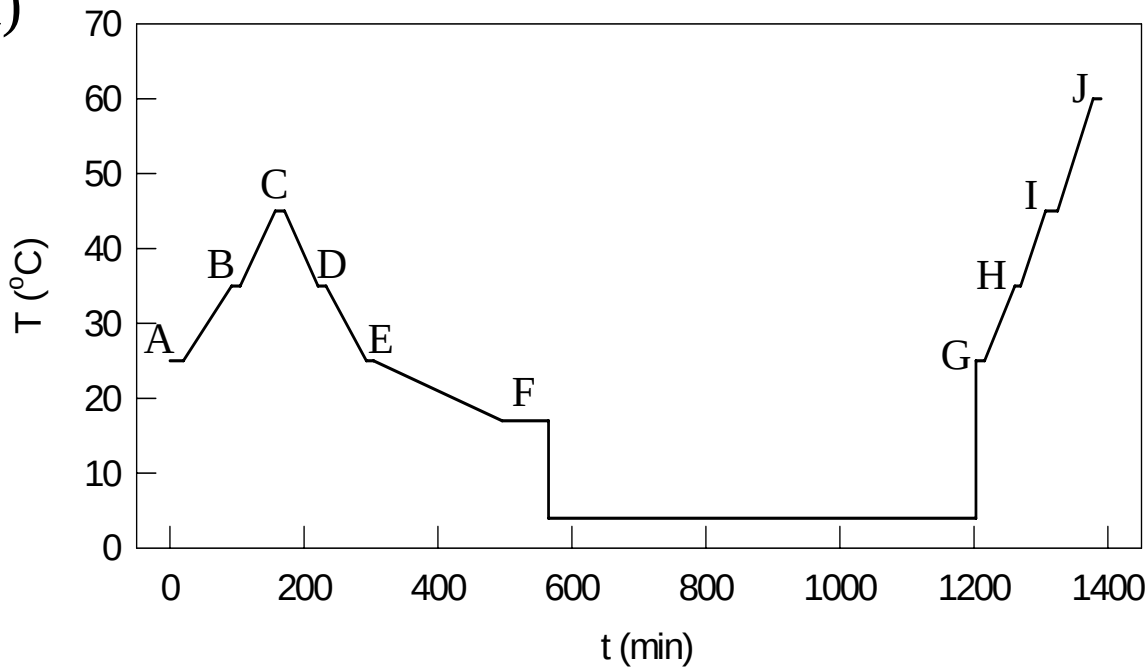
70
60
50
40
30
20
10
0
T (°C)
A
B
C
D
E
F
G
H
I
J
0
200
400
600
800
1000
1200
1400
t (min)

(b)

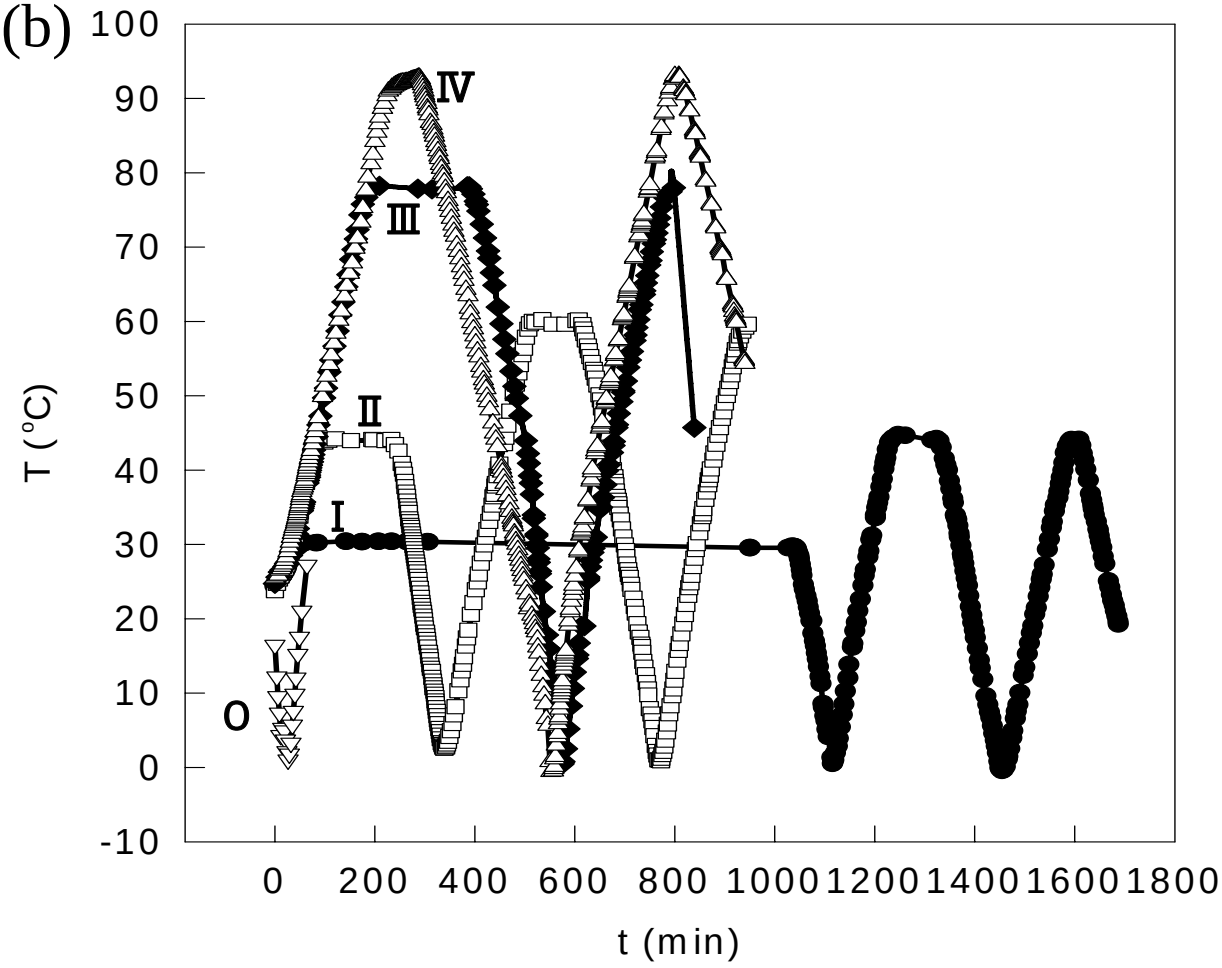
100
90
80
70
60
50
40
30
20
10
0
-10
T (°C)
Ⅳ
Ⅲ
Ⅱ
Ⅰ
O
0
200
400
600
800
1000
1200
1400
1600
1800
t (min)

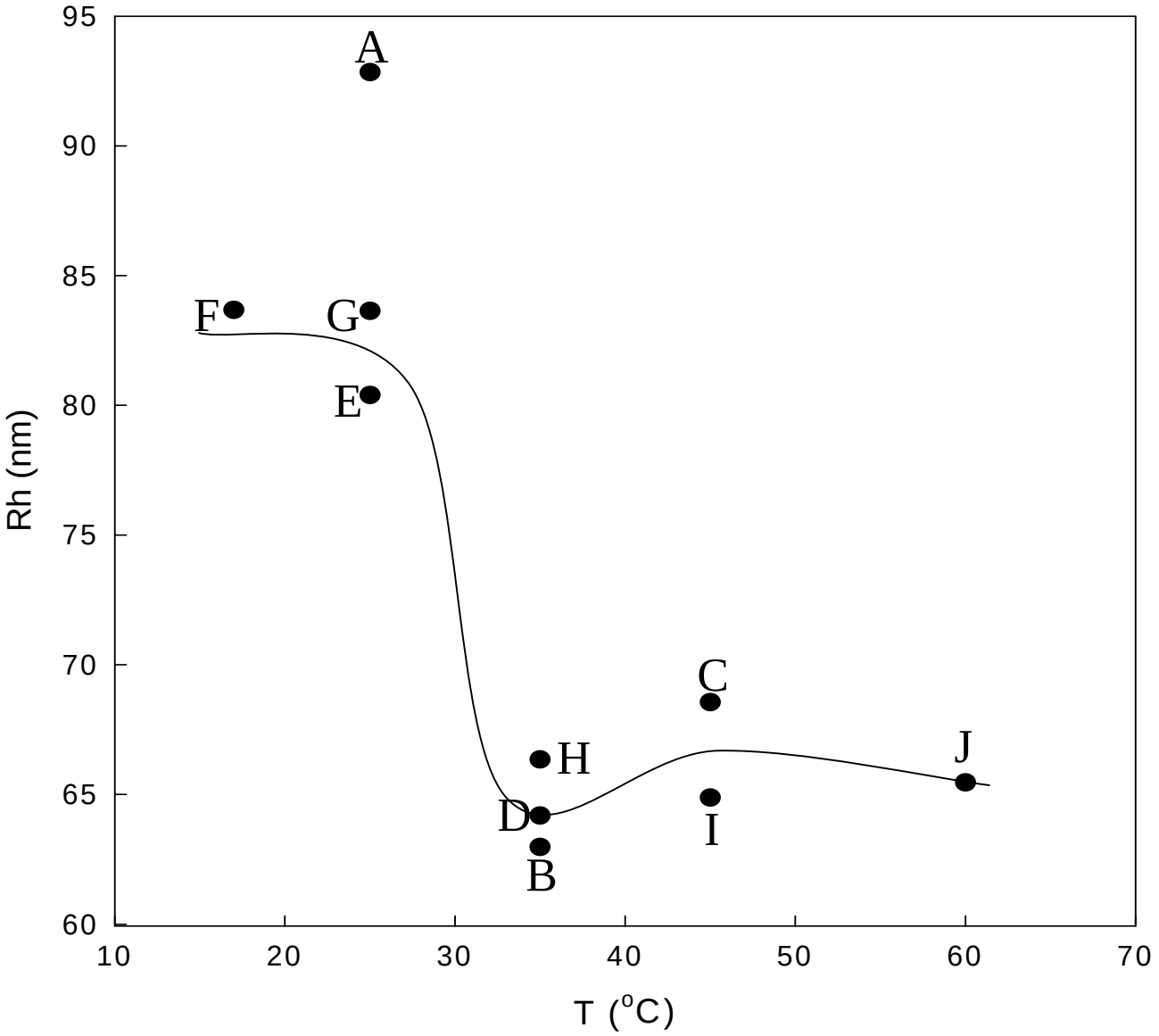
95
90
85
80
75
70
65
60
Rh (nm)
10
20
30
40
50
60
70
T (°C)
A
F
G
E
C
H
J
D
I
B

(a)

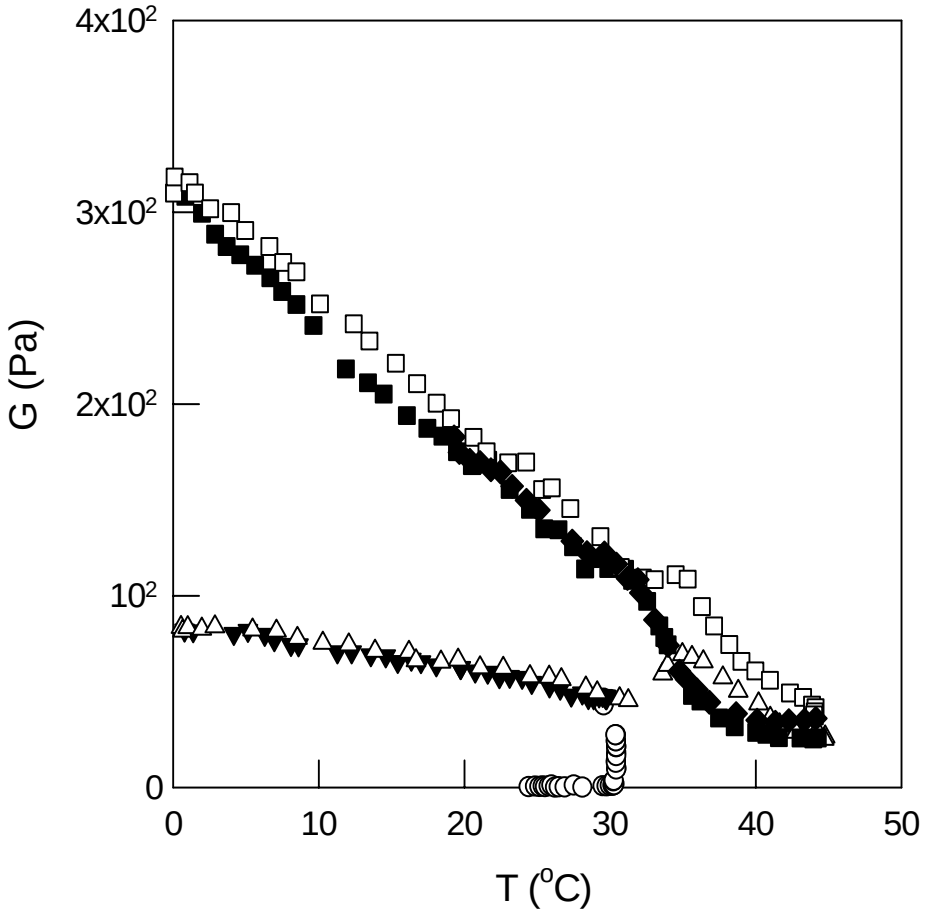
4x10²
3x10²
2x10²
10²
0
G (Pa)
0
10
20
30
40
50
T (°C)

(b)

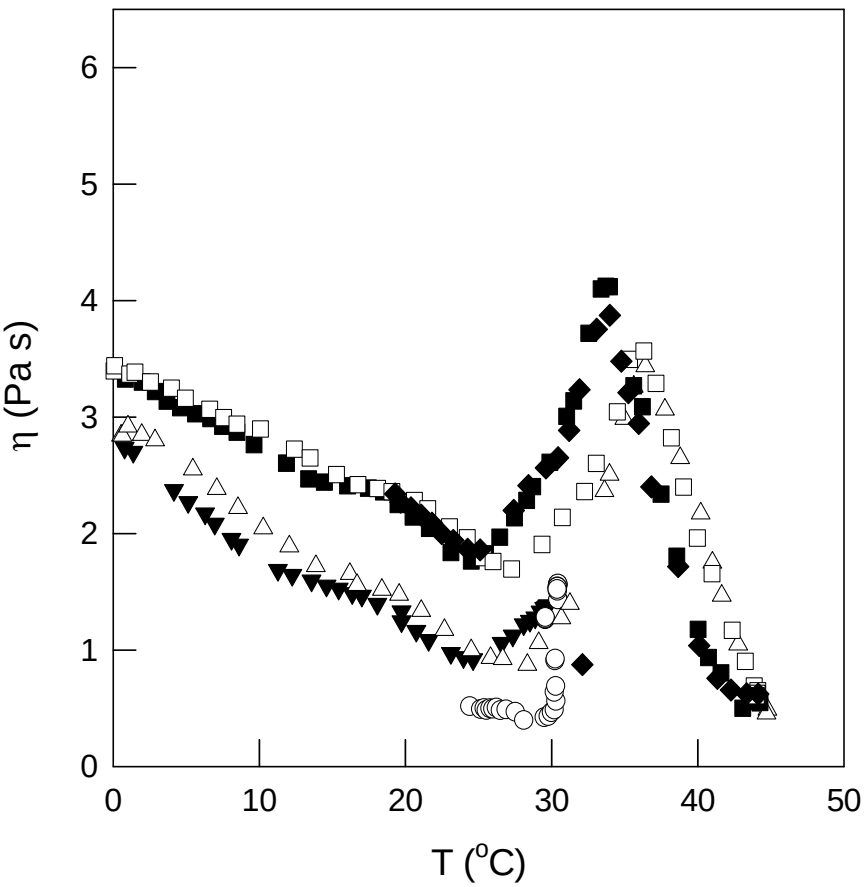
6
5
4
3
2
1
0
η (Pa s)
0
10
20
30
40
50
T (°C)

(a)

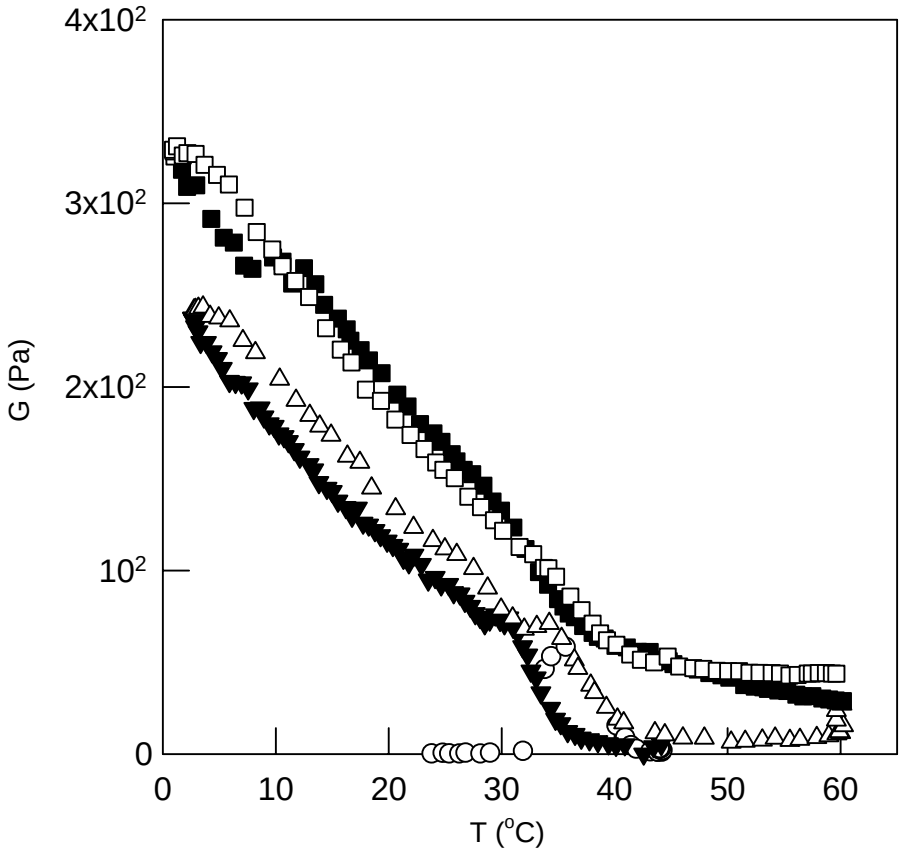
4x10²
3x10²
2x10²
10²
0
G (Pa)
0
10
20
30
40
50
60
T (°C)

(b)

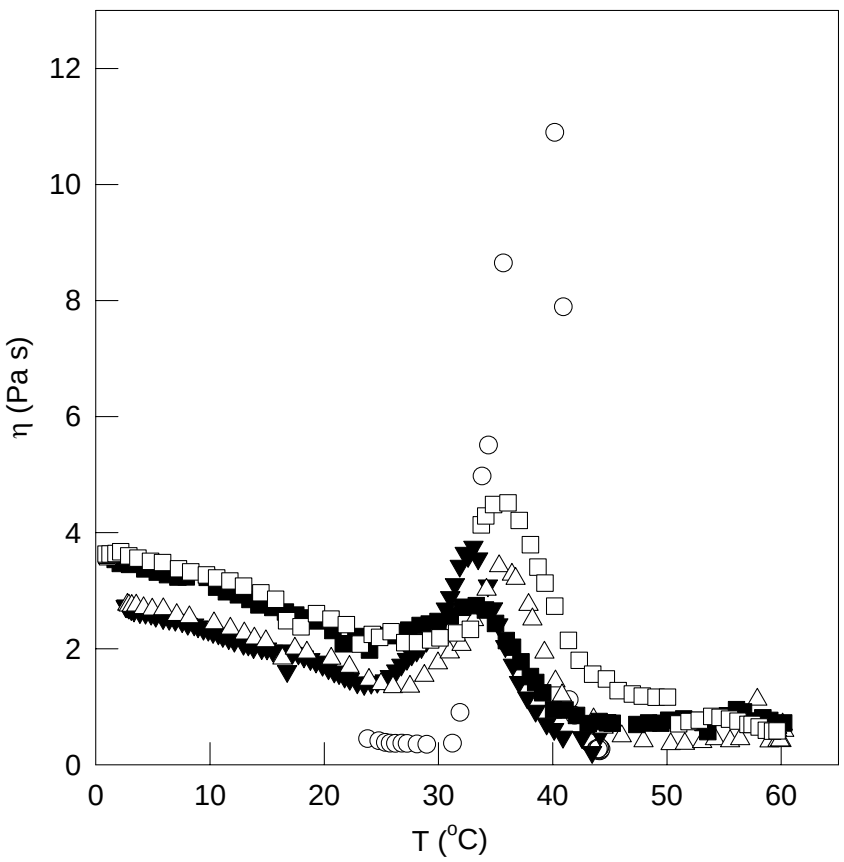
12
10
8
6
4
2
0
η (Pa s)
0
10
20
30
40
50
60
T (°C)

(a)

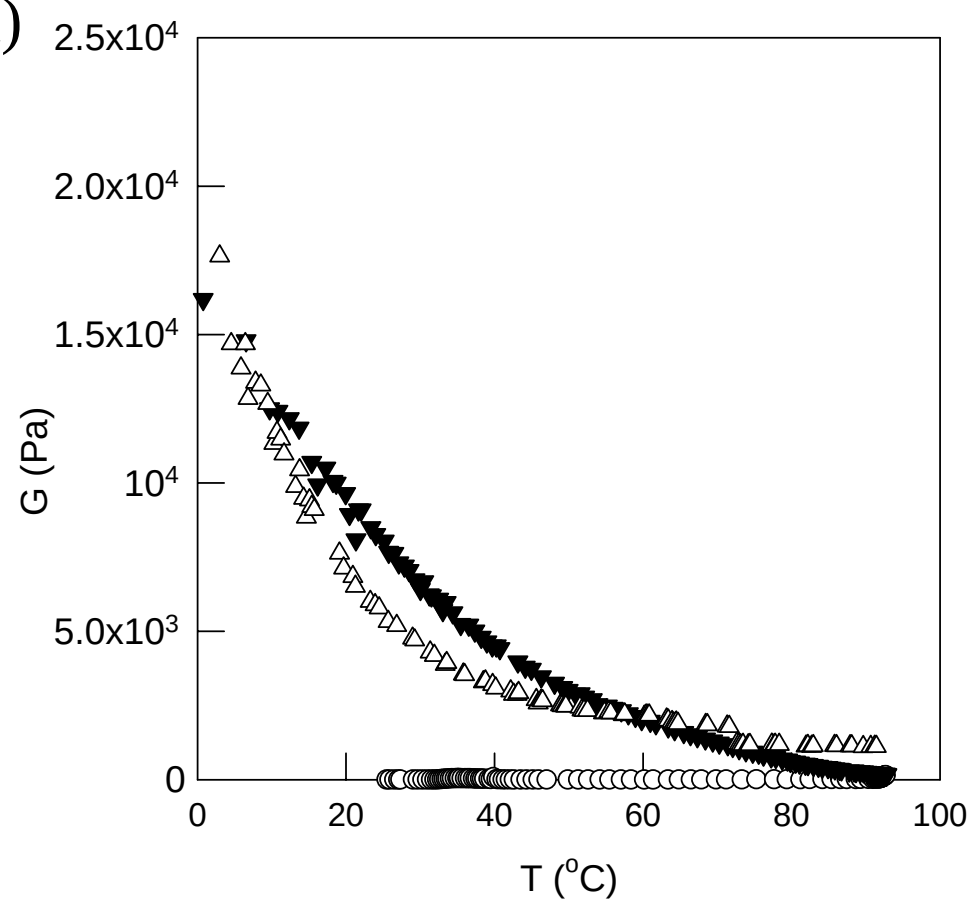
2.5x10^4
2.0x10^4
1.5x10^4
10^4
5.0x10^3
0
G (Pa)
0
20
40
60
80
100
T (°C)

(b)

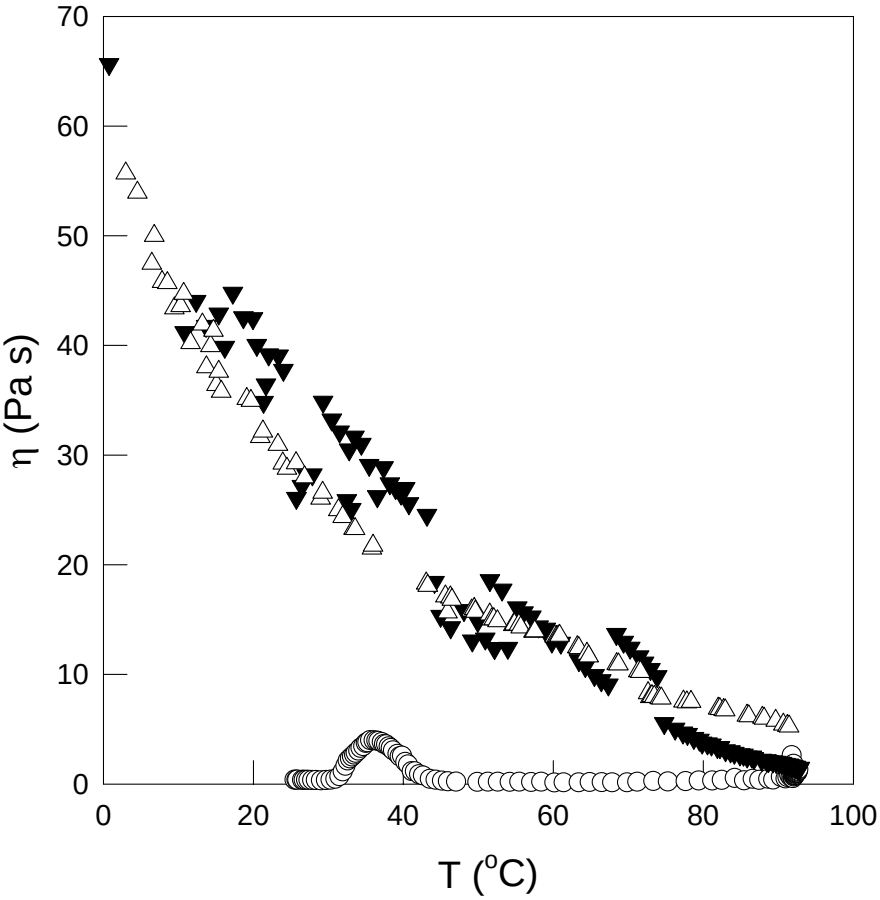
70
60
50
40
30
20
10
0
η (Pa s)
0
20
40
60
80
100
T (°C)

(a)

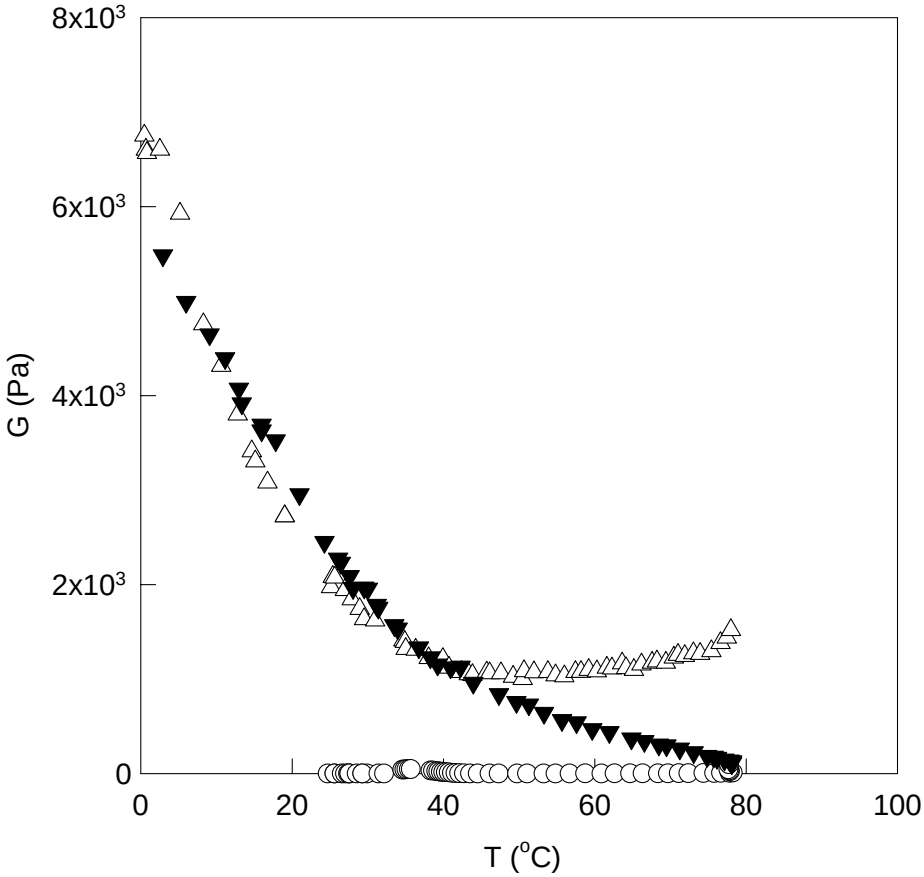
8x10³
6x10³
4x10³
2x10³
0
G (Pa)
0
20
40
60
80
100
T (°C)

(b)

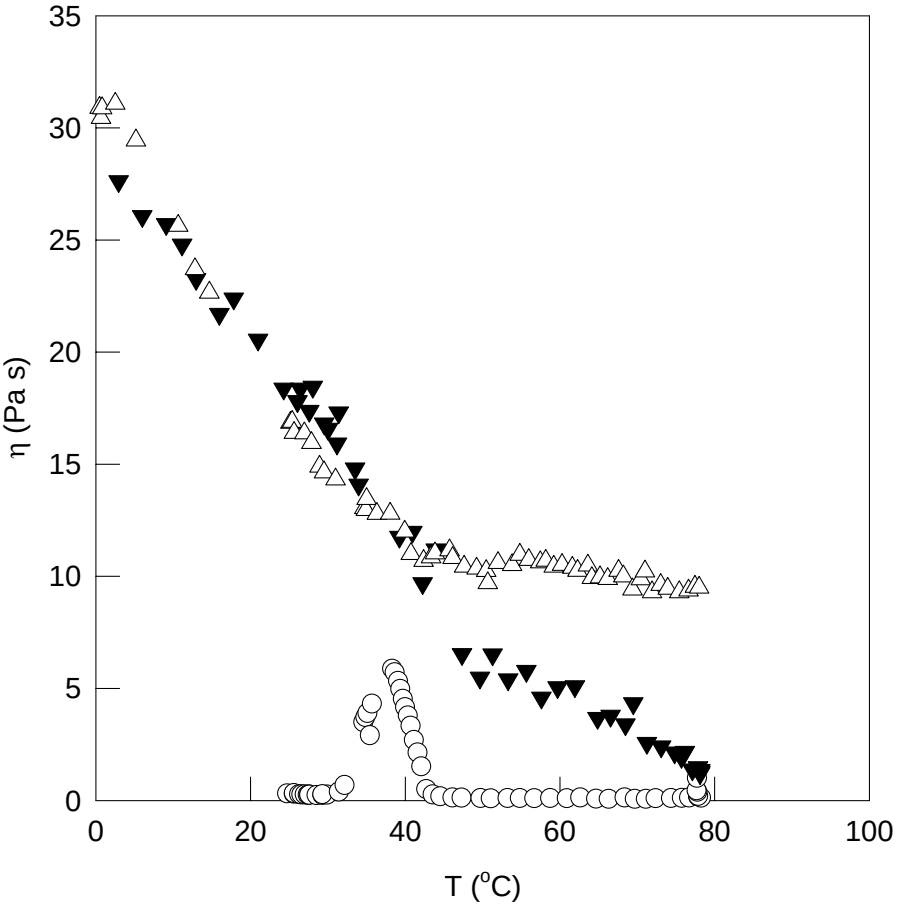
35
30
25
20
15
10
5
0
η (Pa s)
0
20
40
60
80
100
T (°C)

(a)

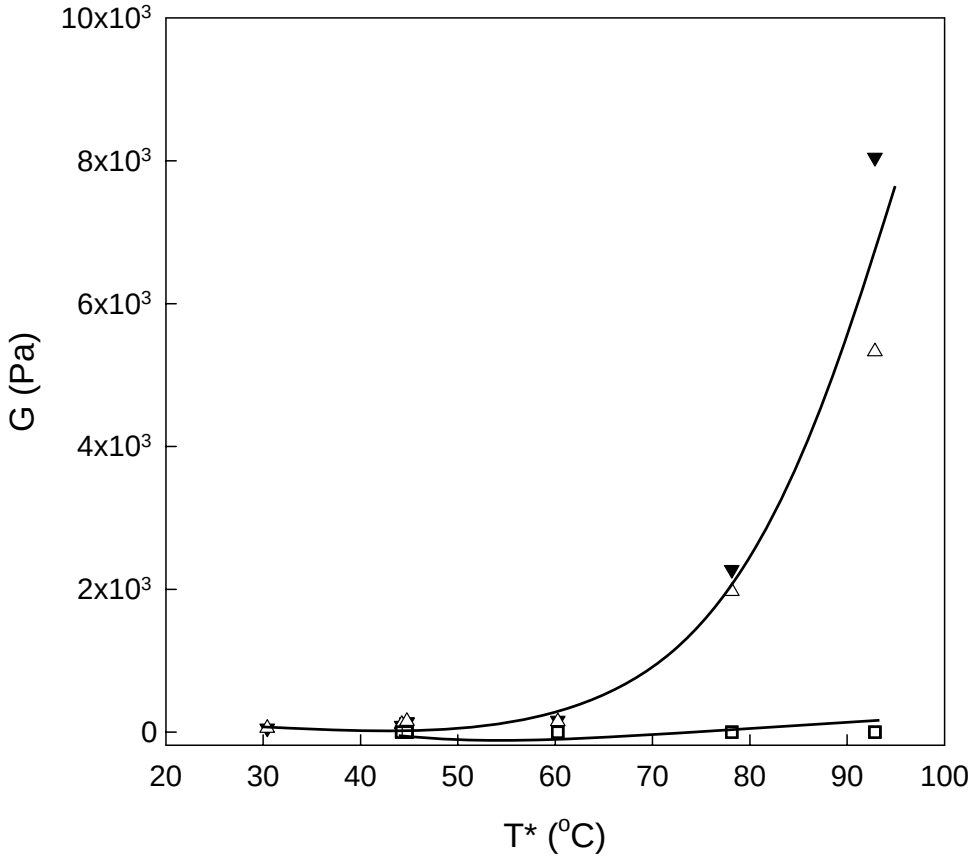
10x10³
8x10³
6x10³
4x10³
2x10³
0
G (Pa)
20
30
40
50
60
70
80
90
100
T* (°C)

(b)

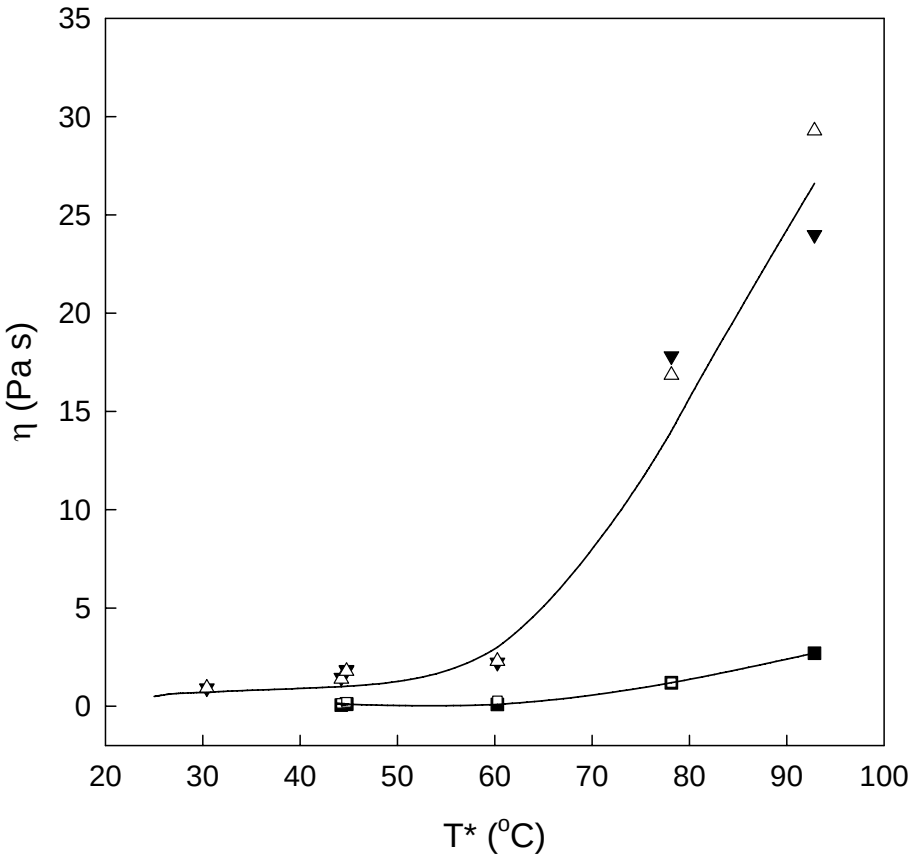
35
30
25
20
15
10
5
0
η (Pa s)
20
30
40
50
60
70
80
90
100
T* (°C)

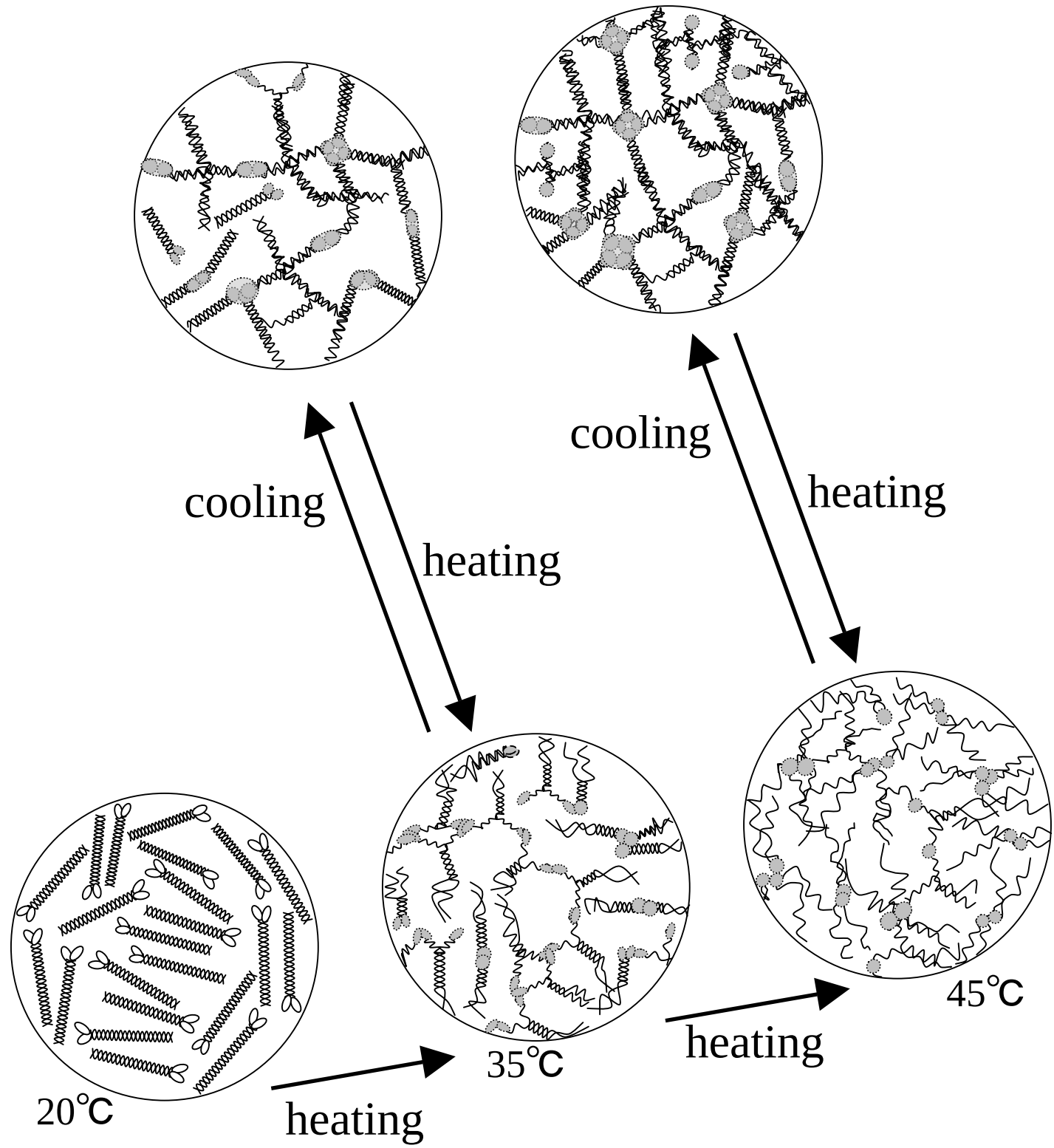
cooling
heating
cooling
heating
20℃
heating
35℃
heating
45℃

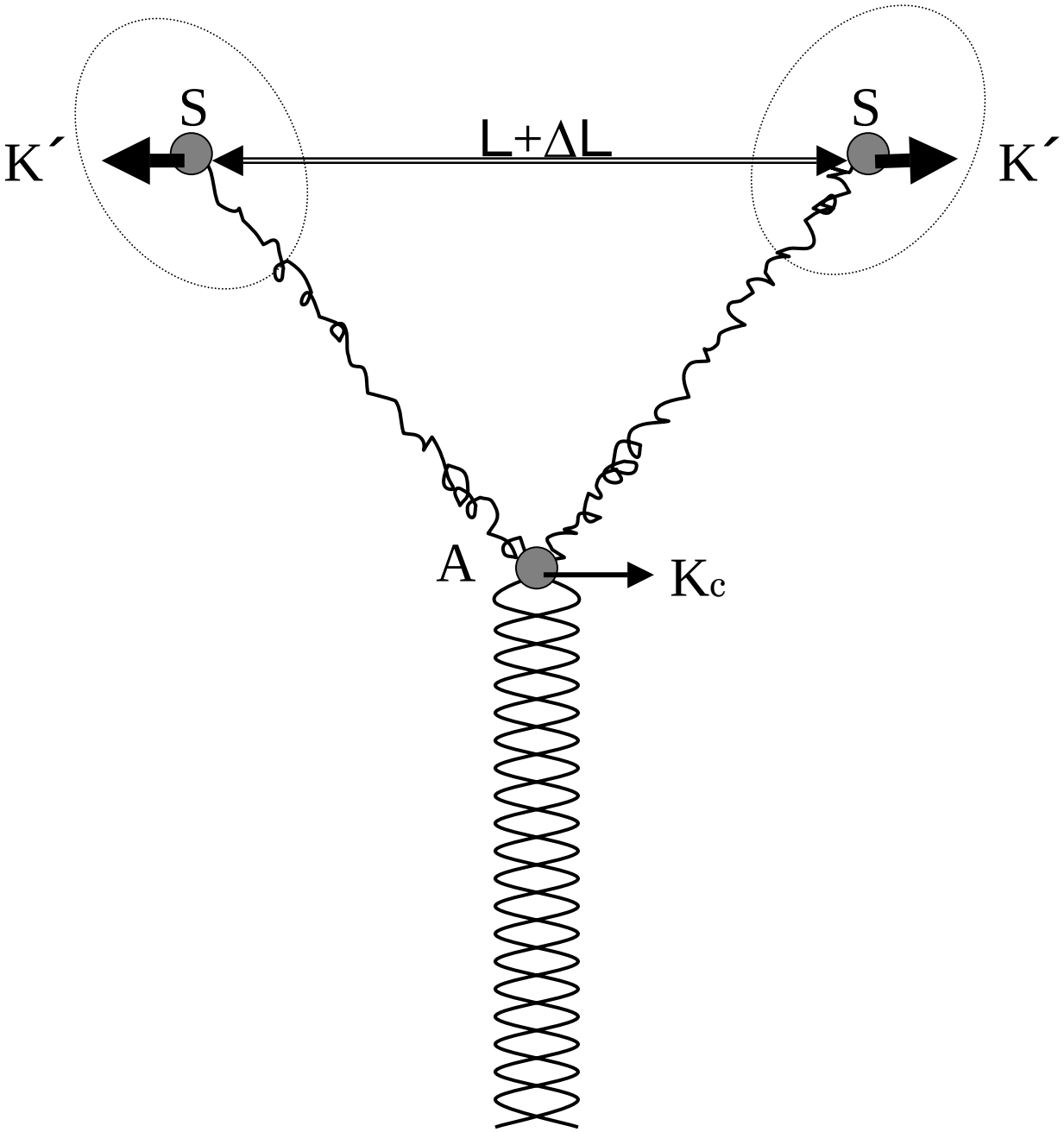
S
S
L+ΔL
K´
K´
A
Kc